# Pairing of Spin Excitations in Lateral Quantum Dots

Marek Korkusiński,[1] Pawel Hawrylak,[1] Mariusz Ciorga,[1] Michel Pioro-Ladrière,[1,2] and Andrew S. Sachrajda[1]

[1]*Institute for Microstructural Sciences, National Research Council of Canada, Ottawa K1A0R6, Canada*

[2]*Département de Physique, Université de Sherbrooke, Sherbrooke, Québec, Canada*

(Received 25 November 2003; published 12 November 2004)

We demonstrate the existence of correlated electronic states as paired spin excitations of lateral quantum dots in the integer quantum Hall regime. Starting from the spin-singlet filling-factor $\nu = 2$ droplet, by increasing the magnetic field we force the electrons to flip spins and increase the spin polarization. We identify the second spin-flip process as one accompanied by correlated, spin depolarized phases, interpreted as pairs of spin excitons. The correlated states are identified experimentally in few-electron lateral quantum dots using high source-drain voltage spectroscopy.

DOI: 10.1103/PhysRevLett.93.206806 PACS numbers: 73.21.La, 73.23.Hk, 85.75.Hh

Pairing of elementary excitations is a signature of electronic correlations in many areas of physics. Good examples are Cooper pairs of electrons in superconductors, correlated pairs of electrons and holes forming biexcitons in semiconductors, and spin excitons forming skyrmions in quantum Hall ferromagnets. In this Letter we predict and observe pairing of spin excitations of few-electron quantum dots in the integer quantum Hall regime. The result of this pairing is that the second spin-flip process, counted from the spin-singlet, filling-factor $\nu = 2$ droplet, is composed of a number of correlated electronic states. The correlated states can be understood as pairs of spin excitons at the edge of a quantum Hall droplet, giving credence to earlier theoretical work [1,2], in particular, that by Tejedor and coworkers [3], and adding correlations to previously identified effects due to direct and exchange interactions in quantum dots [4–9].

To study the second spin flip we use the quantum-dot device in which a controlled number of electrons $N$ can be confined and subjected to a perpendicular magnetic field $\mathbf{B}$ [4]. The single particle energies of the dot, the Fock-Darwin (FD) levels, are those of two harmonic oscillators: $\varepsilon(nm\sigma) = \Omega_+(n + 1/2) + \Omega_-(m + 1/2) + g\mu_B B\sigma$, where $n$, $m$ are the quantum numbers and $\sigma$ is the electronic spin [2]. The oscillator energies are $\Omega_\pm = \Omega_h \pm \omega_c/2$, where $\Omega_h = \sqrt{\omega_0^2 + \omega_c^2/4}$, with $\omega_0$ being the characteristic energy of the confining potential and $\omega_c$, the cyclotron energy. In high magnetic fields $\Omega_+ \gg \Omega_-$, and we may restrict ourselves to the lowest-Landau level (LLL), i.e., we set $n = 0$, and end up with a linear dispersion of energy levels $\varepsilon(m\sigma) = m\Omega_- + g\mu_B B\sigma$ as a function of the angular momentum $l = m$ and spin.

The ground and excited states of a dot filled with $N$ electrons are determined by a competition between kinetic, Zeeman, and Coulomb energies. This competition is described by the Hamiltonian of $N$ interacting electrons

$$\hat{H} = \sum_i \varepsilon(i) c_i^+ c_i + \frac{1}{2}\sum_{ijkl} \langle ij|V|kl\rangle c_i^+ c_j^+ c_k c_l, \qquad (1)$$

where $c_i^+$ ($c_i$) is the electronic creation (annihilation) operator on the FD level $i$ [$i = (m\sigma)$], and $\langle ij|V|kl\rangle$ are the Coulomb scattering matrix elements. For parabolic confinement $\langle ij|V|kl\rangle = \alpha \frac{\sqrt{\pi}}{l_h}\langle ij|v|kl\rangle$, with dimensionless $\langle|v|\rangle$, $l_h = \sqrt{1/\Omega_h}$ (in units of Rydberg and effective Bohr radius, respectively), and $\alpha$ [9,10] reflects deviations from ideal Coulomb interactions due to screening, presence of impurities, finite layer thickness, etc.

While extensive numerical calculations were carried out as a function of the electron number $N$, confining energy, Zeeman energy, and the number of Landau levels [11], the physics can be brought out by examining a model system of $N = 8$ electrons in the lowest-Landau-level approximation. In the absence of interactions ($\alpha = 0$) we distribute equal number of $N_U = 4$ electrons with spin-up and $N_D = 4$ electrons with spin-down on the lowest four FD states: $m = 0, 1, 2, 3$. This compact, spin-singlet, filling-factor $\nu = 2$ state is the ground state over a certain range of values of the magnetic field. As we increase the magnetic field, the kinetic energy spacing $\Omega_-$ decreases, but the Zeeman splitting $E_Z = |g\mu_B B|$ increases. Because of the competition of these two energy scales the number $N_D$ of spin-down electrons increases at the expense of the spin-up electrons in a series of spin flips (SFs). The first SF configuration can be treated as a single exciton with a total angular momentum increase from the $\nu = 2$ state of $L = +1$. The second SF state is composed of two spin-flip excitons, with $L = +1 + 3 = +4$. The magnetic-field evolution of the droplet is qualitatively the same in the presence of the Coulomb interactions ($\alpha = 1$) within the Hartree-Fock approximation. The spin excitons, now composed of quasiparticles, and spin-flip transitions are now driven by interaction effects rather than the Zeeman energy.

Note that the angular momentum of the first spin-flip state is $L = +1$, and that of the second spin-flip state is $L = +4$, which leaves unexplored Hilbert spaces with angular momenta $L = +2$ and $L = +3$. Let us focus on these configurations, starting with $L = +2$. There are three spin-singlet configurations $S_z = 0$, $S = 0$, as shown

  

in Fig. 1. Figures 1(a) and 1(b) are one-electron-hole-pair singlet excitations $|S_1\rangle$ and $|S_2\rangle$. Figure 1(c), on the other hand, involves two electron-hole pairs which form a spin-singlet biexciton. In analogous way we can create two one-electron-hole-pair triplet excitations $|T_1\rangle$, $|T_2\rangle$. We can therefore divide our Hilbert space into two subspaces, a singlet one with three states, and a triplet one with two states. In the LLL approximation all these configurations have the same kinetic energy and the ground state, and hence the total spin, is determined solely by interactions. Not surprisingly, we find that exchange lowers the Hartree-Fock energy of triplet states below the energy of the singlets, including the biexciton state, as shown in the left-hand panel of Fig. 1(d). Including correlations changes the ordering of levels dramatically. The correlated energy levels obtained by diagonalizing the Hamiltonian matrix are shown in the right-hand panel of Fig. 1(d). Correlations among the three singlet states, in particular, the contribution from the biexciton state, overcome the exchange gain of the triplet states and lead to the spin-singlet ground state. The spin-singlet ground state $|G\rangle = A|XX\rangle + B|S_1\rangle + C|S_2\rangle$ is a correlated state, with the $|XX\rangle$ configuration contributing $|A|^2 = 48.5\%$, $|S1\rangle$ contributing $|B|^2 = 31.7\%$, and $|S2\rangle$ contributing $|C|^2 = 19.8\%$ spectral weight. The ground state is dominated by the biexciton configuration.

Let us now turn to the analysis of the angular momentum subspace $L = +3$. In the LLL approximation we can generate here ten configurations with total $S_z = 0$, five with $S_z = -1$, and five with $S_z = +1$. Let us focus on the triplet configurations with $(L, S, S_z) = (+3, 1, -1)$. Out of five configurations possible in this subspace we show the dominant three configurations in Figs. 2(a)–2(c). The first one, $|1\rangle$, is a pair of spin excitons. It differs from the singlet biexciton $|XX\rangle$ configuration with $L = +2$ by having the two holes with parallel spin. It can be interpreted as an "internal spin-flip" configuration. The configuration $|2\rangle$ also consists of a pair of spin excitons, while the other configuration, $|3\rangle$, is a single electron-hole-pair excitation. Upon numerical diagonalization of our simple Hamiltonian we find that the state $|1\rangle$ contributes to the ground state 41.7% spectral weight, while the states $|2\rangle$ and $|3\rangle$ contribute 25.8% and 32.5%, respectively. Hence, the ground state is strongly correlated, with dominant contribution from the internal spin-flip configuration. If all five possible spin triplet configurations are included, the contribution of the state $|1\rangle$ is 44.5%, and of the states $|2\rangle$ and $|3\rangle$ is 27.5% and 25%, respectively, the remaining weight (about 3%) taken by the remaining two configurations. In Fig. 2(d) we show a comparison of the Hartree-Fock energies of the three dominant configurations (the left panel) with the exact energies obtained with the three (middle panel) and all the five configurations (right panel).

We now turn to the evolution of the ground state of the droplet with magnetic field. We start in the regime of magnetic fields in which the ground state of the dot is the $\nu = 2$ configuration, and end when the second SF has occurred. In this region of magnetic fields, the Hartree-Fock approximation predicts only two transitions, the first and the second SF, both driven by direct and exchange

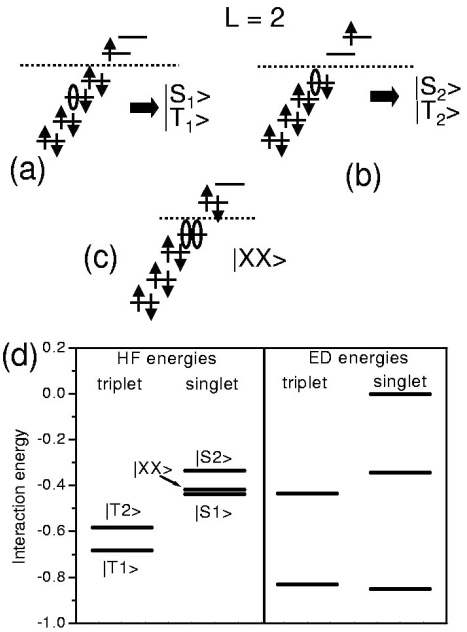


FIG. 1. (a)–(c) Three possible lowest-Landau-level configurations with angular momentum $L = +2$ and $S = 0$. The dashed line denotes the Fermi level. (d) Energies of singlets and triplets with $L = 2$: Hamiltonian diagonal terms (left) and correlated eigenstates (right) (see text).

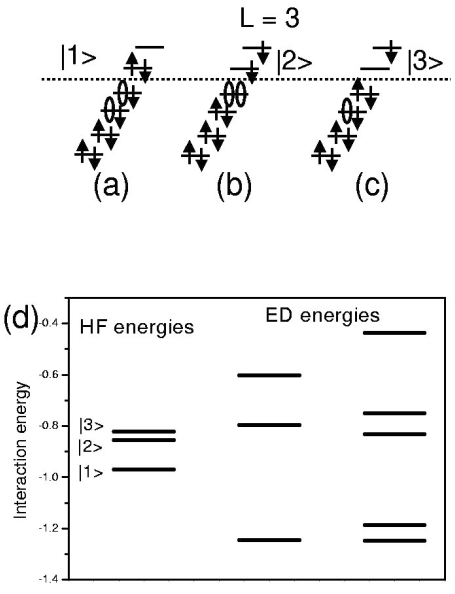


FIG. 2. (a)–(c) Three out of five possible lowest-Landau-level configurations with angular momentum $L = +3$ and $S_z = -1$. The dashed line denotes the Fermi energy. (d) Energies of the $L = +3$ states for three and five states: Hartree-Fock (left), correlated eigenstates with the three-configuration (middle) and the full five-configuration basis (right).

interactions. However, the correlations bring down the energies of $L = +2$ (biexciton) and $L = +3$ (internal SF) states sufficiently for them to become ground states of the system. The evolution of the eight-electron droplet with the magnetic field is thus $L = 0$, singlet $\rightarrow L = +1$, triplet (1SF) $\rightarrow L = +2$, singlet (biexciton) $\rightarrow L = +3$, triplet (internal SF) $\rightarrow L = +4$, spin two (2SF). The charge density corresponding to the sequence of these ground states is shown in Fig. 3(a). The up (down) triangles represent electrons with spin-up (down), and their area is proportional to the calculated charge density. The charge densities well resemble the dominant configurations of the $\nu = 2$ state, 1SF, spin biexciton, internal spin-flip, and 2SF states. This detailed analysis identifies electronic correlations and pairing of spin excitations as the origin of the total spin oscillation across the second SF. Figure 3(b) shows the stability regions of all the phases as a function of the magnetic field and electron number for $\omega_0 = 6$ meV, $E_Z = 0$, $\alpha = 1$ and GaAs material parameters [12]. The $\nu = 2$ phase has a finite stability region, both in magnetic field and in the electron number [13]. For all the electron numbers for which $\nu = 2$ is stable, we find a similar evolution of the droplet: the first SF, followed by the biexciton correlated phase, and finally the second SF. The internal SF phase, however, is stable only for low electron numbers and vanishes for $N > 12$. A detailed discussion of these results, obtained as a function of the strength of Coulomb interactions, confining energy, Zeeman energy, and the number of Landau levels, will be given elsewhere [11].

Because our quantum dot enables us to control the electron number, we can compare theoretical predictions with experiment for exactly the same number of electrons $N = 8$. The layout of the device, as well as relevant experimental details are described elsewhere [14]. We focus here on the high source-and-drain spectroscopy involving tunneling of the eighth electron through the seven-electron dot. The tunneling current, probing the ground and excited states of the eight-electron droplet, is typically recorded as a differential conductance trace. In the main panel of Fig. 4 we show the positions of peaks of the differential conductance in our system as a function of the gate voltage and the magnetic field, while the actual trace for $B = 1.2$ T (i.e., along the dashed line) is shown in the inset.

For a given value of the magnetic field (horizontal axis) we change the gate voltage (vertical axis), thereby shifting the energies of the eight-electron quantum-dot states. When the ground state of the eight-electron dot enters the tunneling window, the current starts to flow, which on the differential plot appears as a positive peak (low-energy edge).

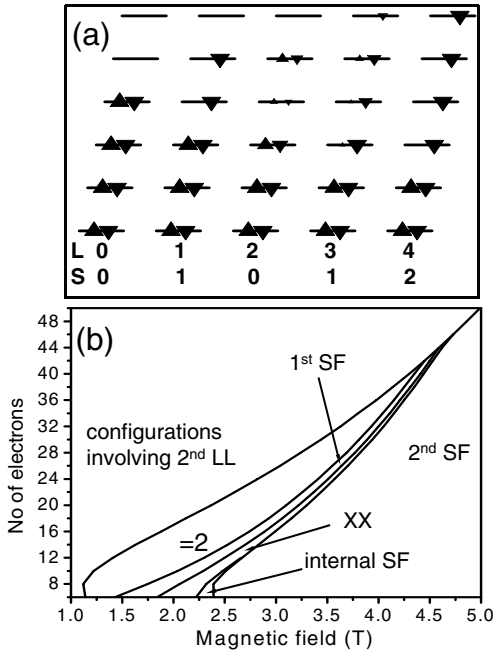


FIG. 3. (a) Charge densities for the states $\nu = 2$, first spin flip, correlated biexciton, internal spin flip, and the second spin flip (from left to right, respectively), calculated within the one-Landau-level approximation. The dashed line denotes the Fermi level. (b) Boundaries between phases of an even-electron droplet as a function of the number of electrons and the magnetic field for $\omega_0 = 6$ meV, $E_Z = 0$.

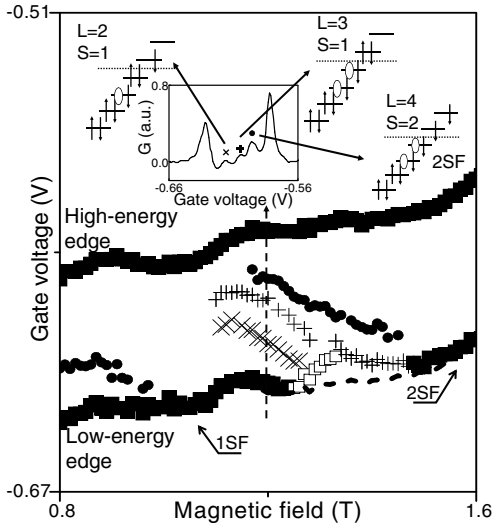


FIG. 4. Main plot: Positions of maxima of the differential conductance tracing the addition spectrum of the eighth electron to a seven-electron dot measured with a lateral gated quantum-dot device in the high source-drain voltage regime. The differential conductance trace for the magnetic field $B = 1.2$ T is shown in the inset. Arrows in the bottom part of the figure indicate the first and the second spin flip. In the vicinity of the second spin flip we interpret the excited states as (from left to right): the correlated triplet (marked by x symbols), the correlated internal spin flip (marked by crosses) and the second spin flip (filled circles); the diagrams show schematically their corresponding charge densities. The empty squares mark the region of the negative differential conductance (see text for details).

Upon further tuning of the gates the excited states enter the window. In each case a new conductivity channel opens up, which shows as higher energy peaks on the trace (marked with filled circles and cross symbols). Finally, for even higher gate voltages, the ground state of the eight-electron dot exits the tunneling window, and the eighth electron can no longer tunnel out of the dot. Therefore, at this point the current cannot flow any more, which result in the final high-energy peak in the spectrum (high-energy edge). For the traces of the ground states, this scenario is valid throughout the entire range of the magnetic field except from 1.25 to 1.5 T. In this region, the trace corresponding to the ground state appears to be missing (the dashed line in Fig. 4 shows our extrapolation of the data). Also, the entry of one of the excited states into the window is accompanied by a *decrease* of the tunneling current, showing on the plot as the negative differential conductance (empty squares). Let us now focus on the other excited states. In the low-field part of the graph ($B \leq 1.05$ T) we see a single excited state of decreasing energy. This state becomes a ground state of the system at $B \approx 1.05$ T. From an independent low source-drain voltage measurement (not shown) we identify this transition as the first spin flip. By contrast, the second spin flip at higher magnetic fields is clearly composed of a band of three excited states.

Let us now interpret the experimental data in terms of the correlated states predicted by our theory. In order to be able to interpret both the position and the amplitude of the observed traces, we first note that the seven-electron droplet remains in the same ground state with total spin $S = 3/2$ throughout the entire complicated second spin flip, i.e., it contains three unpaired spin-down electrons. The amplitude of the tunneling current depends therefore on the total spin of the ground state of the eight-electron dot. In particular, by adding the eighth electron we cannot create a spin singlet (due to the spin blockade), but we can create spin triplets. Now, the first of the three excited states can be identified as the one with quantum numbers $L = +2, S = 1$, and it represents an *excited* state of the $L = 2$ Hilbert space. The spin biexciton $L = +2, S = 0$ ground state, expected at lower energy and lower $B$, is not visible due to the spin blockade. Its becoming the ground state of the system appears to correspond to the disappearance of the ground state at $B \approx 1.25$ T. In accordance with our calculations, the two remaining lines correspond to the correlated internal spin-flip state, $L = +3, S = 1$, and the simple second spin-flip state, $L = +4, S = 2$. The spin blockade does not apply here and both of these states become new ground states terminating the region of negative differential conductance. Unlike the second spin-flip state, however, the internal spin-flip state is correlated and the current amplitude is low. Our model does not fully explain the nature of the negative conductance trace. Preliminary experimental studies suggest that this line is, in fact, a signature of one of the excited states of the seven-electron dot; its entry into the tunneling window combined with the correlated nature of the ground state of the eight-electron dot (which in this regime is the spin biexciton $L = +2, S = 0$) appears to lead to a decrease of the tunneling current.

In conclusion, we demonstrated pairing of spin excitations of few-electron quantum dots in the integer quantum Hall regime. The pairing of spin excitons at the second spin flip of a quantum Hall droplet leads to oscillation of the total spin due to a correlated spin biexciton and internal spin-flip states. The spin exciton states lead to a composite nature of the second spin-flip event. A preliminary report on this work was presented at the QD2002 Conference in Tokyo [14].

P. H. and A. S. thank the Canadian Institute for Advanced Research for partial support. M. K. and M. P-L. thank NSERC and IMS NRC for partial support.

[1] P. A. Maksym and T. Chakraborty, Phys. Rev. Lett. **65**, 108 (1990); P. A. Maksym and T. Chakraborty, Phys. Rev. B **45**, 1947 (1992); J. M. Kinaret *et al.*, Phys. Rev. B **46**, 4681 (1992); P. Hawrylak *et al.*, Phys. Rev. B **59**, 2801 (1999); S.-R. Eric Yang, A. H. MacDonald, and M. D. Johnson, Phys. Rev. Lett. **71**, 3194 (1993); M.-C. Cha and S.-R. Eric Yang, Phys. Rev. B **67**, 205312 (2003); B. Reusch, W. Häusler, and H. Grabert, Phys. Rev. B **63**, 113313 (2001); M. Koskinen, M. Manninen, and S. M. Reimann, Phys. Rev. Lett. **79**, 1389 (1997).

[2] P. Hawrylak, Phys. Rev. Lett. **71**, 3347 (1993); A. Wojs and P. Hawrylak, Phys. Rev. B **56**, 13227 (1997).

[3] J. J. Palacios *et al.*, Phys. Rev. B **50**, 5760 (1994); J. H. Oaknin *et al.*, Phys. Rev. Lett. **74**, 5120 (1995); J. H. Oaknin, L. Martin-Moreno, and C. Tejedor, Phys. Rev. B **54**, 16850 (1996).

[4] S. Tarucha *et al.*, Phys. Rev. Lett. **77**, 3613 (1996); T. H. Oosterkamp *et al.*, Phys. Rev. Lett. **82**, 2931 (1999).

[5] M. Ciorga *et al.*, Phys. Rev. Lett. **88**, 256804 (2002).

[6] S. Tarucha *et al.*, Phys. Rev. Lett. **84**, 2485 (2000).

[7] O. Klein *et al.*, Phys. Rev. Lett. **74**, 785 (1995).

[8] M. Ciorga *et al.*, Physica E (Amsterdam) **11**, 35 (2001); A. S. Sachrajda *et al.*, Physica E (Amsterdam) **10**, 493 (2001).

[9] P. L. McEuen *et al.*, Phys. Rev. B **45**, 11419 (1992).

[10] A. Wojs and P. Hawrylak, Phys. Rev. B **51**, 10880 (1995); M. Eto, Jpn. J. Appl. Phys. **36**, 3924 (1997); J. Kyriakidis *et al.*, Phys. Rev. B **66**, 035320 (2002).

[11] M. Korkusinski and P. Hawrylak (unpublished).

[12] The electronic effective mass $m^* = 0.067\ m_0$, the dielectric constant $\epsilon = 12.4$, and the Landé factor $g = -0.44$ are that of GaAs.

[13] A. Wensauer, M. Korkusinski, and P. Hawrylak, Phys. Rev. B **67**, 035325 (2003).

[14] M. Ciorga *et al.*, Phys. Status Solidi B **238**, 325 (2003).